Author Manuscript

Author Manuscript

Author Manuscript

Author Manuscript

HHS Public Access

Author manuscript

JACC Cardiovasc Imaging. Author manuscript; available in PMC 2022 February 02.

Published in final edited form as:

JACC Cardiovasc Imaging. 2020 July ; 13(7): 1521–1530. doi:10.1016/j.jcmg.2020.01.014.

Prognostic Value of Myocardial Extracellular Volume Fraction and T2-mapping in Heart Transplant Patients

Kongkiat Chaikriangkrai, MD[a,*], **Muhannad Aboud Abbasi, MD**[a,*], **Roberto Sarnari, MD**[a], **Ryan Dolan, MD**[a], **Daniel Lee, MD**[b], **Allen S. Anderson, MD**[b], **Kambiz Ghafourian, MD**[b], **Sadiya S. Khan, MD**[b], **Esther E. Vorovich, MD**[b], **Jonathan D. Rich, MD**[b], **Jane E. Wilcox, MD**[b], **Julie A. Blaisdell, MS**[a], **Clyde W. Yancy, MD**[b], **James Carr, MD**[a], **Michael Markl, PHD**[a]

[a]Department of Radiology, Feinberg School of Medicine, Northwestern University, Chicago, Illinois

[b]Division of Cardiology, Department of Medicine, Northwestern University, Chicago, Illinois

Abstract

OBJECTIVES—To examine prognostic value of T1- and T2-mapping techniques in heart transplant patients.

BACKGROUND—Myocardial characterization using T2 mapping (evaluation of edema/inflammation) and pre- and post-gadolinium contrast T1 mapping (calculation of extracellular volume fraction [ECV] for assessment of interstitial expansion/fibrosis) are emerging modalities that have been investigated in various cardiomyopathies.

METHODS—A total of 99 heart transplant patients underwent the magnetic resonance imaging (MRI) scans including T1- (n = 90) and T2-mapping (n = 79) techniques. Relevant clinical characteristics, MRI parameters including late gadolinium enhancement (LGE), and invasive hemodynamics were collected. Median clinical follow-up duration after the baseline scan was 2.4 to 3.5 years. Clinical outcomes include cardiac events (cardiac death, myocardial infarction, coronary revascularization, and heart failure hospitalization), noncardiac death and noncardiac hospitalization.

RESULTS—Overall, the global native T1, postcontrast T1, ECV, and T2 were 1,030 ± 56 ms, 458 ± 84 ms, 27 ± 4% and 50 ± 4 ms, respectively. Top-tercile-range ECV (ECV >29%) independently predicted adverse clinical outcomes compared with bottom-tercile-range ECV (ECV <25%) (hazard ratio [HR]: 2.87; 95% confidence interval [CI]: 1.07 to 7.68; p = 0.04) in a multivariable model with left ventricular end-systolic volume and LGE. Higher T2 (T2 ≥50.2 ms) independently predicted adverse clinical outcomes (HR: 3.01; 95% CI: 1.39 to 6.54; p = 0.005) after adjustment for left ventricular ejection fraction, left ventricular end-systolic volume, and LGE. Additionally, higher T2 (T2 ≥50.2 ms) also independently predicted cardiac events (HR: 4.92; CI: 1.60 to 15.14; p = 0.005) in a multivariable model with left ventricular ejection fraction.

ADDRESS FOR CORRESPONDENCE: Dr. Kongkiat Chaikriangkrai, Department of Radiology, Northwestern University, 737 North Michigan Avenue, Suite 1600, Chicago, Illinois 60611. supersoon@gmail.com. Twitter: @SoonKongkiat.

*Drs. Chaikriangkrai and Abbasi contributed equally to this work

Author Manuscript Author Manuscript Author Manuscript Author Manuscript

CONCLUSIONS—MRI-derived myocardial ECV and T2 mapping in heart transplant patients were independently associated with cardiac and noncardiac outcomes. Our findings highlight the need for larger prospective studies.

Keywords

extracellular volume fraction; heart transplantation; magnetic resonance imaging; natural history; prognosis; T1 mapping; T2 mapping

Cardiovascular magnetic resonance imaging (CMR) with myocardial characterization by late gadolinium enhancement (LGE) has become an established prognostic imaging modality in various cardiovascular diseases (1–5). LGE has been shown to have a strong correlation with focal or regional myocardial fibrosis (6,7) in pathological specimens and portends worse prognosis in various patient populations (1–5). However, myocardial characterization by LGE imaging relies on contrast agent uptake in scar tissue relative to normal or “remote” myocardium. This approach is limited in patients with diffuse myocardial changes without discernable normal myocardium, a situation commonly encountered in myocardial diseases. Advances in cardiac magnetic resonance imaging (MRI) have enabled further myocardial characterization by parametric T1 and T2 mapping including the calculation of extracellular volume fraction (ECV) from pre- and post-gadolinium contrast T1 mapping. These methods quantify myocardial changes without the need of normal myocardium and are thus suitable for assessing diffuse changes of the myocardium in patients with various cardiovascular conditions. Factors affecting native T1 and T2 can be in either intracellular or extracellular spaces. Increased water (edema and/or inflammatory changes) and fat content (e.g., cardiac lipoma, sphingolipid in Fabry disease) lengthens both native T1 and T2. Native T1 is also affected by protein (e.g., amyloid proteins), fibrosis, and paramagnetic substances (e.g., gadolinium, iron). On the other hand, ECV is a surrogate for extracellular space that can be affected by myocyte hypertrophy (e.g., athlete’s heart), fibrosis, water (edema), and protein deposition (8).

T1 and T2 mapping have been shown to have prognostic value in a spectrum of cardiomyopathies (9–15). Recently, T1 and T2 mapping have been studied in relatively small cohorts of orthotopic heart transplant (OHT) recipients primarily for diagnostic accuracy for acute cardiac allograft rejection (ACR) (16–23). Nevertheless, prognostic evaluation of these techniques in OHT patients is lacking. The objective of this study was to examine prognostic value of T1- and T2-mapping markers in OHT patients.

METHODS

STUDY DESIGN AND PATIENT SELECTION.

This is a single-center observational prospective cohort study in OHT patients from August 2014 to March 2019. The study was approved by the institutional review board and written informed consent was obtained from all patients. Inclusion criteria were all adult OHT patients 18 to 89 years of age at our hospital. The study patients had a baseline CMR and follow-up scans. Patients were excluded if they had contraindications to CMR (i.e.,

Author Manuscript Author Manuscript Author Manuscript Author Manuscript

pacemakers, aneurysm clips, or shrapnel fragments) or if they were unwilling/unable to give written informed consent.

There were 114 patients enrolled in the study. After excluding 15 patients because of consent withdraw (n = 5) and incomplete T1-mapping data (n = 10 with only native T1 mapping), the patients were categorized into 2 cohorts. The objective of the first cohort (n = 90) was to evaluate the prognostic value of T1 mapping and therefore included patients who had native and postcontrast T1-mapping data. The objective of the second cohort (n = 79) was to evaluate the prognostic value of T2 mapping beyond prediction of ACR (any antibody-mediated rejection or grade >2R acute cellular rejection). To avoid potential confounding effect of ACR on prognosis, patients within their first year of OHT (n = 20) or patients who had proven ACR episode 1 month before/after the CMR scan (n = 2) were not included in this cohort.

CMR PROTOCOL.

All studies were carried out on a 1.5-T MRI scanner (Magnetom, Espree, and Avanto, Siemens Healthcare, Erlangen, Germany). The CMR protocol consisted of cine steady-state free-precession (SSFP) and LGE sequences performed in matching short- and long-axis planes. Short-axis images were acquired every 1 cm (gap, 4 mm) throughout the entire heart. Breath-held segmented cine SSFP was carried out with the following typical parameters: repetition time repetition time (TR) = 3.0 ms; echo time (TE) = 1.5 ms; flip angle 70°, field of view 250 × 350, matrix 150 × 192, slice thickness 6 mm, and temporal resolution 35 to 40 ms. LGE images were obtained during breath hold using a segmented inversion-recovery sequence (in-plane spatial resolution 1.8 × 1.3 mm, slice thickness 6 mm; temporal resolution 160 to 200 ms) 10 to 15 min after intravenous contrast administration (gadobutrol, 0.2 mmol/kg). Inversion times were adjusted to null viable myocardium.

T1 mapping was performed using a modified Look-Locker inversion recovery technique as described previously (24). Short-axis slices were acquired during breath-hold before and 15 to 25 min following the intravenous administration of the contrast agent bolus. Imaging reconstruction included motion correction of the modified Look-Locker inversion images with different inversion times, and the calculation of parametric left ventricular (LV) T1 maps. T1-mapping acquisition parameters were as follows: spatial resolution (pixel size) 1 to 1.4 × 1 to 1.4 mm^2, slice thickness 8 mm, TE/TR 1.0 to 1.3 ms/2.0 to 2.2 ms; flip angle 35°. Patient hematocrit was collected immediately before the CMR exam.

T2-mapping was based on the successive acquisition of three T2-prepared SSFP images with varying T2-prep times (0, 24, 55 ms). Further imaging parameters were as follows: TE = 1.1 to 1.4 ms, TR = 2.2 to 2.6 ms, spatial resolution = 1.5 to 2.1 mm × 2.0 to 2.5 mm, slice thickness = 8 mm, diastolic acquisition window = 270 ms, flip angle = 70°.

CMR DATA ANALYSIS.

Cine SSFP data were used to quantify global cardiac function parameters. LV and right ventricular (RV) volumes were measured by planimetry of the endocardial borders on a stack of short-axis images. Papillary muscles and trabeculae were included as part of the blood pool on the contours. LV end-diastolic volume, LV end-systolic volume, RV

Author Manuscript Author Manuscript Author Manuscript Author Manuscript

end-diastolic volume, and RV end-systolic volume were calculated by summation of these images. LV ejection fraction and RV ejection fraction were determined by subtracting the end-systolic volumes from the end-diastolic volumes and dividing the result by end-diastolic volumes. Presence of LGE was assessed qualitatively.

Native T1, T2, and postcontrast T1 values were calculated based on the American Heart Association 16-segment model using manual contouring of the LV epicardium/endocardium. Additionally, native and postcontrast regions of interest were drawn in the LV blood pool cavity. All the analysis was performed with CVI42 (Circle Cardiovascular Imaging, Calgary, Ontario, Canada). ECV was calculated with the following formula: ECV = (Δ[1/T1myocardium]/Δ[1/T1blood pool]) × [1 - hematocrit]). Δ represents the difference between the postcontrast and native T1 values. Global native, postcontrast T1 mapping, and ECV were calculated as the average of all available segmental T1-mapping values (25) from the basal and mid slices because we have noted systematically lower native T1 and higher ECV values in the apical segments compared with the basal and mid segments possibly because of partial volume effects.

CLINICAL EVENTS DATA COLLECTION.

Baseline and follow-up characteristics were retrieved on the day of the baseline and follow-up CMR scans by dedicated research study personnel and they include patient demographics, comorbidities, history of ACR (26), current medications, and cardiac catheterization data.

Clinical events in this study were a composite of all death, nonfatal myocardial infarction (NFMI), coronary revascularization, and all unplanned hospitalization. Cardiac events were defined as a composite of cardiac death, NFMI, coronary revascularization, and heart failure hospitalization. The diagnosis of NFMI was defined as chest pain associated with a troponin I ≥0.10 ng/dl. Follow-up clinical events were collected by review of medical records. All OHT patients in our hospital were cared and communicated closely by the OHT team including visit, electronic message, and telephone communications.

STATISTICAL ANALYSIS.

Descriptive statistics for studied variables are presented as mean ± SD for normally distributed continuous variables, median (interquartile range[IQR]) for non-normally distributed continuous variables and frequency with percentage for categorical variables. Continuous variables were compared between 2 groups with independent-samples Student's *t*-test (normally distributed), Mann-Whitney *U* test (non-normally distributed), among 3 groups with analysis of variance and chi-square test for categorical data. T1- and T2-mapping data were analyzed as continuous and categorical variables. T1-mapping data in the same patient over time were compared using paired-samples Student's *t*-test.

Cumulative clinical events as a function of time was investigated using Kaplan-Meier curve analysis. To assess influence of T1- and T2-mapping data on clinical outcomes, univariable and multivariable Cox regression analysis was used. All independent variables with $p < 0.10$ in univariable analysis were considered to be included into a multivariable Cox regression model. Variables with the lowest p value had higher priority to be included first. The

Author Manuscript Author Manuscript Author Manuscript Author Manuscript

number of independent variables included in the multivariable model was constrained to yield roughly 10 events per variable to avoid invalidity of the model (27). For independent variables with significant multicollinearity (defined as a variance inflation factor of >3), only 1 independent variable with the lowest p value was included in multivariable analysis. The risk of overfitting the model was investigated with the Akaike information criterion. The regression analysis results are presented as hazard ratios (HRs) and 95% confidence intervals (CIs). All statistical analysis was performed with IBM SPSS/PASW Statistics 23 (SPSS Inc., Chicago, Illinois). All tests were 2-tailed with $p < 0.05$ considered statistically significant.

RESULTS

PATIENT AND CMR CHARACTERISTICS.

The final T1-mapping cohort comprised 90 patients with the OHT-baseline CMR interval of 5.1 years (IQR: 2.0 to 8.0 years). The median interval between invasive hemodynamics and the baseline CMR was 0.5 month (IQR: 1 to 12 months). The final T2-mapping cohort comprised 79 patients with the OHT-baseline CMR interval of 6.3 years (IQR: 3.9 to 8.7 years). The median interval between invasive hemodynamics and CMR was 5 weeks (IQR: 1 to 13 weeks).

Baseline clinical and CMR characteristics categorized by ECV tercile and T2 values are shown in Table 1. Overall, the global native T1, postcontrast T1, and ECV were 1,030 ± 56 ms, 458 ± 84 ms, and 27 ± 4%, respectively. Global T2 was 50 ± 4 ms.

NATURAL HISTORY OF T1 AND ECV.

There were 44 (49%) patients who had 1 follow-up CMR after the baseline CMR. The interval between the baseline CMR and the follow-up CMR was 13 months (IQR: 10 to 23 months). In this subgroup of patients who had follow-up CMR, the global native T1, postcontrast T1 and ECV were 1,022 ± 452 ms, 483 ± 93 ms, and 27 ± 4%, respectively. At follow-up, only postcontrast T1 significantly decreased from the baseline CMR as shown in Figure 1. There was no significant change in native T1 or ECV noted at follow-up scans.

PROGNOSTIC IMPLICATION OF T1 AND ECV.

Median follow-up duration for clinical events after the baseline scans was 2.4 years (IQR: 1.6 to 3.5 years). Clinical events occurred in 32 patients (36%), including 3 deaths (1 cardiogenic shock, 1 septic shock, 1 saddle pulmonary embolism), 6 heart failure hospitalizations, 3 percutaneous coronary interventions, and 20 non-cardiac hospitalization (17 infection-related hospitalization including pneumonia, urinary tract infection, abdominal infection, cellulitis, bacteremia, and 3 non-infection-related hospitalization including venous thromboembolism, bowel perforation, and spinal cord compression). Clinical events occurred 2.1 years (IQR: 1.4 to 2.8 years) after the baseline CMR. Patients who had clinical events had significantly higher prevalence of baseline LGE (53 vs. 26%; $p = 0.01$) with higher pulmonary capillary wedge pressure (PCWP) (16 ± 7 mm Hg vs. 12 ± 7 mm Hg; $p = 0.03$), RV (36 ± 10 mm Hg vs. 30 ± 8 mm Hg; $p = 0.009$) and right atrial (RA) pressures (12

Author Manuscript Author Manuscript Author Manuscript Author Manuscript

± 7 mm Hg vs. 8 ± 5 mm Hg; p = 0.008). Accuracy of ECV >29% for prediction of clinical outcomes is shown in Table 2.

Univariable Cox analysis showed significant association between clinical events and higher ECV compared with the bottom-range group, presence of LGE, larger LV end-systolic volume index (LVESVI), higher RA pressure, higher RV pressures, and higher pulmonary pressures. Multivariable analysis adjusted for presence of LGE and LVESVI demonstrates independent association of higher clinical event incidence with the top-range ECV compared with the bottom-range ECV (HR: 2.87; 95% CI: 1.07 to 7.68; p = 0.04) and presence of LGE (HR: 2.40; 95% CI: 1.19 to 4.85; p = 0.02) (Table 3). Adding ECV to LGE extent in the multivariable model improved predictivity of the model with borderline significance (global chi-square improved from 7 to 13 with p = 0.05). Adjusted survival curve categorized by myocardial ECV is shown in the Central Illustration. Multivariable analysis adjusted for significant invasive hemodynamics demonstrates independent association of higher clinical event incidence with higher PCWP but not with ECV (Table 3).

There was no significant difference in incidence of cardiac events among the ECV groups (10% vs. 9% vs. 14% in the bottom-range, mid-range, and top-range groups, respectively; p = 0.685). Univariable analysis did not reveal significant association between higher ECV groups and cardiac events (top-range group HR: 1.95; 95% CI: 0.44 to 8.74; p = 0.38 compared with the bottom-range group).

PROGNOSTIC IMPLICATION OF T2 MAPPING.

Median follow-up duration was 3.5 years (IQR: 2.0 to 4.0 years) from the CMR scan. Clinical events occurred in 38 patients (48%), which include 18 cardiac events (3 deaths from cardiogenic shock, 12 heart failure hospitalizations, 3 percutaneous coronary interventions) and 20 noncardiac hospitalization. In those who had cardiac events, the median interval between the CMR and the cardiac event was 1.9 years (IQR: 0.9 to 2.8 years). Patients who developed events had significantly higher mean global T2 (53 ± 4 ms vs. 50 ± 4 ms; p = 0.004), higher PCWP (18 ± 9 mm Hg vs. 12 ± 6 mm Hg; p = 0.01), mean RA pressure (13 ± 7 mm Hg vs. 8 ± 5 mm Hg; p = 0.04), PA diastolic pressure (17 ± 9 mm Hg vs. 13 ± 6 mm Hg; p = 0.05), larger LVESVI (31 ± 6 ml/m^2 vs. 24 ± 7 ml/m^2; p = 0.01), and lower LVEF (52 ± 10% vs. 58 ± 7%; p = 0.004). Accuracy of T2 >50.2 ms for prediction of clinical outcomes are shown in Table 2.

Univariable Cox regression analysis showed significant association of cardiac events with higher native T1, higher T2, larger LVESVI, lower LVEF, higher RA pressure, and pulmonary pressures. Multivariable analysis adjusted for significant CMR finding demonstrates independent association of higher clinical event with both higher T2 and lower LVEF as shown in Table 4. Multivariable analysis adjusted for significant invasive hemodynamic demonstrates independent association of higher cardiac event incidence with both higher T2 and higher PCWP. Adding T2 to LVEF or PCWP in the multivariable models significantly improved predictivity of the models (global chi-square improved from 11 to 21 with p = 0.02 and from 13 to 20 with p = 0.01, respectively). Adjusted survival curve categorized by T2 is shown in the Central Illustration.

Author Manuscript Author Manuscript Author Manuscript Author Manuscript

Higher T2 was also significantly associated with higher all clinical event rate in the univariable analysis (HR: 2.5; 95% CI: 1.3 to 5.0; p = 0.009). Other variables associated with all clinical events were lower LVEF, larger LVESVI, presence of LGE, higher PCWP, and higher RA, RV, and PA pressures). Multivariable analysis adjusted for significant CMR finding demonstrates independent association of higher clinical event with only higher T2 (Table 4). Multivariable analysis adjusted for significant invasive hemodynamic demonstrates independent association of higher cardiac event incidence with both higher T2 and higher PCWP (Table 4). Adding T2 to other significant CMR findings or invasive hemodynamics in the multivariable models significantly improved predictivity of the models (global chi-square improved from 9 to 17 with p = 0.003 and from 7 to 16 with p = 0.007, respectively).

PROGNOSTIC IMPLICATION OF BOTH ECV AND T2 MAPPING.

In the subset of 70 patients who had both ECV and T2-mapping data, multivariable analysis of ECV and T2 showed significant association of cardiac events with higher T2 (HR: 3.75; 95% CI: 1.01 to 13.91; p = 0.049) but not ECV (HR for ECV 25% to 29%: 1.54; 95% CI: 0.60 to 3.95; p = 0.37, HR for ECV >29%: 2.52; 95% CI: 0.95 to 6.71; p = 0.07). Similarly, multivariable analysis of ECV, T2, LVEF, and LVESVI showed significant association of all clinical events with higher T2 (HR: 2.38; 95% CI: 1.03 to 5.50; p = 0.042) but not ECV (HR for ECV 25% to 29%: 1.53; 95% CI: 0.58 to 4.01; p = 0.39, HR for ECV >29%: 2.15; 95% CI: 0.77 to 5.99; p = 0.14).

DISCUSSION

Detection of myocardial changes with CMR-derived T1- and T2-mapping techniques has been demonstrated in patients with ischemic and nonischemic cardiomyopathies including cardiac amyloidosis, hypertrophic cardiomyopathy, acute myocarditis, and Anderson-Fabry disease (9,10,12,28–32). Both techniques have also been shown to have prognostic values in these populations (9–15). Major CMR societies recommend the use of T1- and T2-mapping markers in certain clinical scenarios (33). In OHT populations, application of CMR has been described for structures and function assessment as well as myocardial characterization. Previous literature has demonstrated myocardial characterization with LGE imaging and its prognosis in this population (34–37). However, because of an innate limitation of LGE techniques, diffuse myocardial changes may be missed. Recently, contemporary T1- and T2-mapping techniques have been examined in OHT population (16–22). Both ECV and T2 have been shown to be higher in OHT patients compared with healthy controls (16) and correlate well with myocardial edema marker (17,21). ECV was also shown to correlate with histological fibrosis (18). Clinically, previous research has demonstrated possible association of higher ECV and T2 with ACR episodes (23). Nevertheless, the prognostic value of T1- and T2-mapping markers has not been established in OHT population.

Our study demonstrates that higher ECV during the baseline CMR assessment predicts overall adverse clinical events. We did not find significant association specifically between T1-mapping markers and adverse cardiac events. This association may suggest potential multifactorial causes of higher ECV in OHT patients. Higher baseline ECV in OHT

Author Manuscript Author Manuscript Author Manuscript Author Manuscript

patients possibly represents all cumulative myocardial insults before the baseline CMR scan including harvesting/transplantation surgery and prior infections, hemodynamic disturbance, and medications. We also found that both ECV and presence of LGE remain independently associated with adverse events after adjustment with other significant clinical characteristics and CMR findings. However, ECV became insignificant after adjustment with invasive hemodynamics. This finding supports ECV, in addition to LGE, as a promising noninvasive prognosticator in OHT patients.

Higher myocardial T2 was associated with adverse overall clinical and cardiac events in our cohort. These associations highlight the clinical importance and implications of myocardial edema. Prolonged myocardial edema and inflammation can cause decreased ventricular compliance and increased stiffness (38,39), eventually resulting in irreversible cardiac structural alterations, ventricular dysfunction, and fibrosis (40). We may speculate that increased T2 values in OHT beyond the first year after OHT is related to repetitive inflammatory events including subtle biopsy negative ACR episodes (41), diffuse low-grade vasculitis component secondary to undetected CAV, which has been previously suggested by histological studies (42), or myocardial edema from congestion of the cardiac allograft as suggested by associations between increased T2 and several right heart/pulmonary invasive hemodynamic data in our study and as shown in prior literature (43).

Furthermore, our work indicates that native T1 and ECV did not change during the 13-month follow-up CMR interval, which is consistent with the lack of association between the CMR-OHT time interval and the baseline T1-mapping markers. The findings may suggest that the myocardial changes (possibly interstitial fibrosis) detected by T1-mapping markers occurred earlier after OHT and did not change significantly afterward.

STUDY LIMITATIONS.

There are some limitations to our study. Our data were from a single-center prospective study. Multicenter larger studies with standardized diagnostic protocols are needed to confirm these findings. Our follow-up interval of T1-mapping cohort was 13 months; therefore, changes or plateau in T1-mapping markers after the follow-up period is possible. Most patients in our studies did not have longer term CMR follow-up scans to evaluate long term change of T1-mapping markers. Last, some relevant clinical information (e.g., prior significant infections and other cardiac biomarkers such as troponins and invasive hemodynamic parameters at closer dates to the baseline and follow-up CMR) and CMR findings (e.g., CMR-derived myocardial strain and myocardial perfusion reserve) were not available for analysis. Reduced myocardial perfusion reserve index and early diastolic strain rate as potential better surrogate markers of cardiac allograft function were found to be associated with cardiac allograft vasculopathy and adverse clinical outcomes (44,45).

CONCLUSIONS

In conclusion, we demonstrate independent association of higher baseline myocardial ECV and T2 with adverse clinical and cardiac events after adjustment in multivariable models. Our findings serve as a pilot study for larger research to evaluate the role of ECV and T2 as noninvasive prognostic markers in OHT population.

Author Manuscript Author Manuscript Author Manuscript Author Manuscript

Acknowledgments

Supported by the National Institutes of Health, National Heart, Lung, and Blood Institute grant R01 HL117888. The authors have reported that they have no relationships relevant to the contents of this paper to disclose.

ABBREVIATIONS AND ACRONYMS

ACR	acute cardiac allograft rejection
CI	confidence interval
CMR	cardiovascular magnetic resonance imaging
ECV	extracellular volume fraction
HR	hazard ratio
LGE	late gadolinium enhancement
LV	left ventricular
LVESVI	left ventricular end-systolic volume index
MRI	magnetic resonance imaging
NFMI	nonfatal myocardial infarction
OHT	orthotropic heart transplant
PCWP	pulmonary capillary wedge pressure
RA	right atrial
RV	right ventricular
SSFP	steady-state free precession
TE	echo time
TR	repetition time

REFERENCES

1. Di Marco A, Anguera I, Schmitt M, et al. Late gadolinium enhancement and the risk for ventricular arrhythmias or sudden death in dilated cardiomyopathy: systematic review and meta-analysis. J Am Coll Cardiol HF 2017;5:28–38.
2. Fontana M, Pica S, Reant P, et al. Prognostic value of late gadolinium enhancement cardiovascular magnetic resonance in cardiac amyloidosis. Circulation 2015;132:1570–9. [PubMed: 26362631]
3. Green JJ, Berger JS, Kramer CM, Salerno M. Prognostic value of late gadolinium enhancement in clinical outcomes for hypertrophic cardiomyopathy. J Am Coll Cardiol Cardiol Img 2012;5: 370–7.
4. Kim RJ, Wu E, Rafael A, et al. The use of contrast-enhanced magnetic resonance imaging to identify reversible myocardial dysfunction. N Engl J Med 2000;343:1445–53. [PubMed: 11078769]
5. Kuruvilla S, Adenaw N, Katwal AB, Lipinski MJ, Kramer CM, Salerno M. Late gadolinium enhancement on cardiac magnetic resonance predicts adverse cardiovascular outcomes in nonischemic cardiomyopathy: a systematic review and meta-analysis. Circ Cardiovasc Imaging 2014;7:250–8. [PubMed: 24363358]

Author Manuscript Author Manuscript Author Manuscript Author Manuscript

6. Hashimura H, Kimura F, Ishibashi-Ueda H, et al. Radiologic-pathologic correlation of primary and secondary cardiomyopathies: MR imaging and histopathologic findings in hearts from autopsy and transplantation. Radiographics 2017;37: 719–36. [PubMed: 28129067]
7. Iles LM, Ellims AH, Llewellyn H, et al. Histological validation of cardiac magnetic resonance analysis of regional and diffuse interstitial myocardial fibrosis. Eur Heart J Cardiovasc Imaging 2015;16:14–22. [PubMed: 25354866]
8. Robinson AA, Chow K, Salerno M. Myocardial T1 and ECV measurement: underlying concepts and technical considerations. J Am Coll Cardiol Cardiol Img 2019;12:2332–44.
9. Avanesov M, Munch J, Weinrich J, et al. Prediction of the estimated 5-year risk of sudden cardiac death and syncope or non-sustained ventricular tachycardia in patients with hypertrophic cardiomyopathy using late gadolinium enhancement and extracellular volume CMR. Eur Radiol 2017;27:5136–45. [PubMed: 28616729]
10. Banypersad SM, Fontana M, Maestrini V, et al. T1 mapping and survival in systemic light-chain amyloidosis. Eur Heart J 2015;36:244–51. [PubMed: 25411195]
11. Kammerlander AA, Marzluf BA, Zotter-Tufaro C, et al. T1 Mapping by CMR imaging: from histological validation to clinical implication. J Am Coll Cardiol Cardiol Img 2016;9:14–23.
12. Wong TC, Piehler K, Meier CG, et al. Association between extracellular matrix expansion quantified by cardiovascular magnetic resonance and short-term mortality. Circulation 2012;126: 1206–16. [PubMed: 22851543]
13. Kotecha T, Martinez-Naharro A, Treibel TA, et al. Myocardial edema and prognosis in amyloidosis. J Am Coll Cardiol 2018;71:2919–31. [PubMed: 29929616]
14. Spieker M, Haberkorn S, Gastl M, et al. Abnormal T2 mapping cardiovascular magnetic resonance correlates with adverse clinical outcome in patients with suspected acute myocarditis. J Cardiovasc Magn Reson 2017;19:38. [PubMed: 28351402]
15. Zia MI, Roifman I, Ghugre NR, et al. Prognostic value of myocardial T2 mapping post reperfused acute myocardial infarction. J Cardiovasc Magn Reson 2015;17:P150.
16. Coelho-Filho OR, Shah R, Lavagnoli CFR, et al. Myocardial tissue remodeling after orthotopic heart transplantation: a pilot cardiac magnetic resonance study. Int J Cardiovasc Imaging 2018; 34:15–24. [PubMed: 27437924]
17. Dolan RS, Rahsepar AA, Blaisdell J, et al. Cardiac structure-function MRI in patients after heart transplantation. J Magn Reson Imaging 2019;49: 678–87. [PubMed: 30142237]
18. Ide S, Riesenkampff E, Chiasson DA, et al. Histological validation of cardiovascular magnetic resonance T1 mapping markers of myocardial fibrosis in paediatric heart transplant recipients. J Cardiovasc Magn Reson 2017;19:10. [PubMed: 28143545]
19. Miller CA, Naish JH, Shaw SM, et al. Multiparametric cardiovascular magnetic resonance surveillance of acute cardiac allograft rejection and characterisation of transplantation-associated myocardial injury: a pilot study. J Cardiovasc Magn Reson 2014;16:52. [PubMed: 25160654]
20. Vermes E, Pantaleon C, Auvet A, et al. Cardiovascular magnetic resonance in heart transplant patients: diagnostic value of quantitative tissue markers: T2 mapping and extracellular volume fraction, for acute rejection diagnosis. J Cardiovasc Magn Reson 2018;20:59. [PubMed: 30153847]
21. Yuan Y, Cai J, Cui Y, et al. CMR-derived extracellular volume fraction (ECV) in asymptomatic heart transplant recipients: correlations with clinical features and myocardial edema. Int J Cardiovasc Imaging 2018;34:1959–67. [PubMed: 30056496]
22. Usman AA, Taimen K, Wasielewski M, et al. Cardiac magnetic resonance T2 mapping in the monitoring and follow-up of acute cardiac transplant rejection: a pilot study. Circ Cardiovasc Imaging 2012;5:782–90. [PubMed: 23071145]
23. Dolan RS, Rahsepar AA, Blaisdell J, et al. Multiparametric cardiac magnetic resonance imaging can detect acute cardiac allograft rejection after heart transplantation. J Am Coll Cardiol Img 2019;12:1632–41.
24. Kellman P, Wilson JR, Xue H, Ugander M, Arai AE. Extracellular volume fraction mapping in the myocardium, part 1: evaluation of an automated method. J Cardiovasc Magn Reson 2012;14:63. [PubMed: 22963517]

Author Manuscript Author Manuscript Author Manuscript Author Manuscript

25. Moon JC, Messroghli DR, Kellman P, et al. Myocardial T1 mapping and extracellular volume quantification: a Society for Cardiovascular Magnetic Resonance (SCMR) and CMR Working Group of the European Society of Cardiology consensus statement. J Cardiovasc Magn Reson 2013;15:92. [PubMed: 24124732]
26. Stewart S, Winters GL, Fishbein MC, et al. Revision of the 1990 working formulation for the standardization of nomenclature in the diagnosis of heart rejection. J Heart Lung Transplant 2005;24:1710–20. [PubMed: 16297770]
27. Peduzzi P, Concato J, Feinstein AR, Holford TR. Importance of events per independent variable in proportional hazards regression analysis. II. Accuracy and precision of regression estimates. J Clin Epidemiol 1995;48:1503–10. [PubMed: 8543964]
28. Bulluck H, Hammond-Haley M, Fontana M, et al. Quantification of both the area-at-risk and acute myocardial infarct size in ST-segment elevation myocardial infarction using T1-mapping. J Cardiovasc Magn Reson 2017;19:57. [PubMed: 28764773]
29. Ferreira VM, Piechnik SK, Dall'Armellina E, et al. T(1) mapping for the diagnosis of acute myocarditis using CMR: comparison to T2-weighted and late gadolinium enhanced imaging. J Am Coll Cardiol Img 2013;6:1048–58.
30. Hinojar R, Varma N, Child N, et al. T1 mapping in discrimination of hypertrophic phenotypes: hypertensive heart disease and hypertrophic cardiomyopathy: findings from the InternationaL T1 Multicenter Cardiovascular Magnetic Resonance Study. Circ Cardiovasc Imaging 2015;8.
31. Karamitsos TD, Piechnik SK, Banypersad SM, et al. Noncontrast T1 mapping for the diagnosis of cardiac amyloidosis. J Am Coll Cardiol Img 2013;6:488–97.
32. Sado DM, White SK, Piechnik SK, et al. Identification and assessment of Anderson-Fabry disease by cardiovascular magnetic resonance noncontrast myocardial T1 mapping. Circ Cardiovasc Imaging 2013;6:392–8. [PubMed: 23564562]
33. Messroghli DR, Moon JC, Ferreira VM, et al. Clinical recommendations for cardiovascular magnetic resonance mapping of T1, T2, T2* and extracellular volume: a consensus statement by the Society for Cardiovascular Magnetic Resonance (SCMR) endorsed by the European Association for Cardiovascular Imaging (EACVI). J Cardiovasc Magn Reson 2017;19:75. [PubMed: 28992817]
34. Butler CR, Kim DH, Chow K, et al. Cardiovascular MRI predicts 5-year adverse clinical outcome in heart transplant recipients. Am J Transplant 2014;14:2055–61. [PubMed: 25100504]
35. Butler CR, Kumar A, Toma M, et al. Late gadolinium enhancement in cardiac transplant patients is associated with adverse ventricular functional parameters and clinical outcomes. Can J Cardiol 2013;29:1076–83. [PubMed: 23380296]
36. Pedrotti P, Vittori C, Facchetti R, et al. Prognostic impact of late gadolinium enhancement in the risk stratification of heart transplant patients. Eur Heart J Cardiovasc Imaging 2017;18:130–7. [PubMed: 27625368]
37. Chaikriangkrai K, Abbasi MA, Sarnari R, et al. Natural history of myocardial late gadolinium enhancement predicts adverse clinical events in heart transplant recipients. J Am Coll Cardiol Img 2019;12:2092–4.
38. Dongaonkar RM, Stewart RH, Geissler HJ, Laine GA. Myocardial microvascular permeability, interstitial oedema, and compromised cardiac function. Cardiovasc Res 2010;87:331–9. [PubMed: 20472566]
39. Pogatsa G, Dubecz E, Gabor G. The role of myocardial edema in the left ventricular diastolic stiffness. Basic Res Cardiol 1976;71:263–9. [PubMed: 938438]
40. Laine GA, Allen SJ. Left ventricular myocardial edema. Lymph flow, interstitial fibrosis, and cardiac function. Circ Res 1991;68:1713–21. [PubMed: 2036720]
41. Tang Z, Kobashigawa J, Rafiei M, Stern LK, Hamilton M. The natural history of biopsy-negative rejection after heart transplantation. J Transplant 2013;2013:236720. [PubMed: 24490053]
42. Lee MS, Tadwalkar RV, Fearon WF, et al. Cardiac allograft vasculopathy: a review. Catheter Cardiovasc Interv 2018;92:E527–36. [PubMed: 30265435]
43. Verbrugge FH, Bertrand P6B, Willems E, et al. Global myocardial oedema in advanced decompensated heart failure. Eur Heart J Cardiovasc Imaging 2017;18:787–94. [PubMed: 27378769]

Author Manuscript Author Manuscript Author Manuscript Author Manuscript

44. Erbel C, Mukhammadaminova N, Gleissner CA, et al. Myocardial perfusion reserve and strain-encoded CMR for evaluation of cardiac allograft microvasculopathy. J Am Coll Cardiol Img 2016;9:255–66.

45. Korosoglou G, Osman NF, Dengler TJ, et al. Strain-encoded cardiac magnetic resonance for the evaluation of chronic allograft vasculopathy in transplant recipients. Am J Transplant 2009;9:2587–96. [PubMed: 19843034]

Author Manuscript Author Manuscript Author Manuscript Author Manuscript

PERSPECTIVES

COMPETENCY IN MEDICAL KNOWLEDGE:

Myocardial characterization is 1 of the main strengths of MRI compared with other cardiac imaging modalities. MRI-derived T1- and T2-mapping techniques have been examined for prognostic value in heart transplant patients in our study. Myocardial characterization using MRI-derived T1- and T2-mapping techniques may have an advantage over a conventional LGE technique especially for the detection of diffuse myocardial changes because this technique does not require normal myocardial reference.

TRANSLATIONAL OUTLOOK:

This is a relatively short-term, small-cohort study. Longer term follow-up with larger cohorts will be needed to better understand the prognostic value of myocardial characterization using MRI-derived T1- and T2-mapping techniques.

Author Manuscript Author Manuscript Author Manuscript Author Manuscript

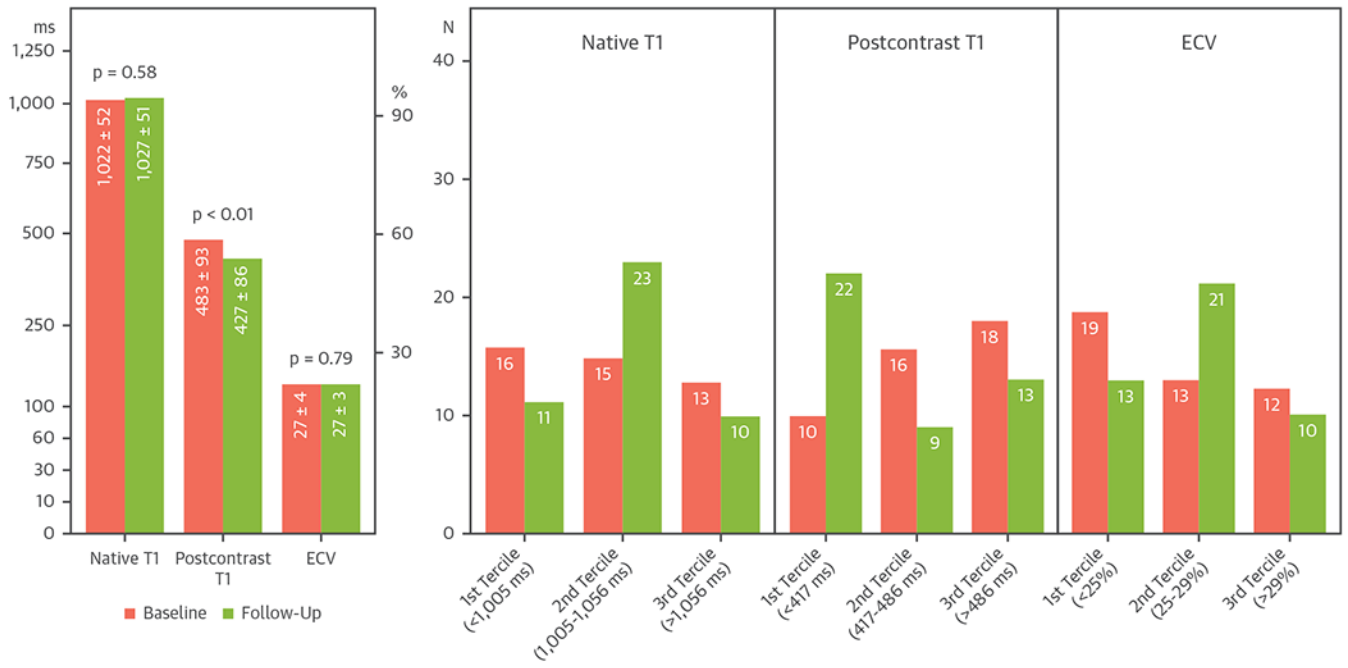

FIGURE 1. Baseline and Follow-Up

T1-mapping values were shown as mean global native T1, postcontrast T1, and extracellular volume fraction (ECV) in the **left panel** and as tercile categories in the **right panels.**

Author Manuscript
Author Manuscript
Author Manuscript
Author Manuscript

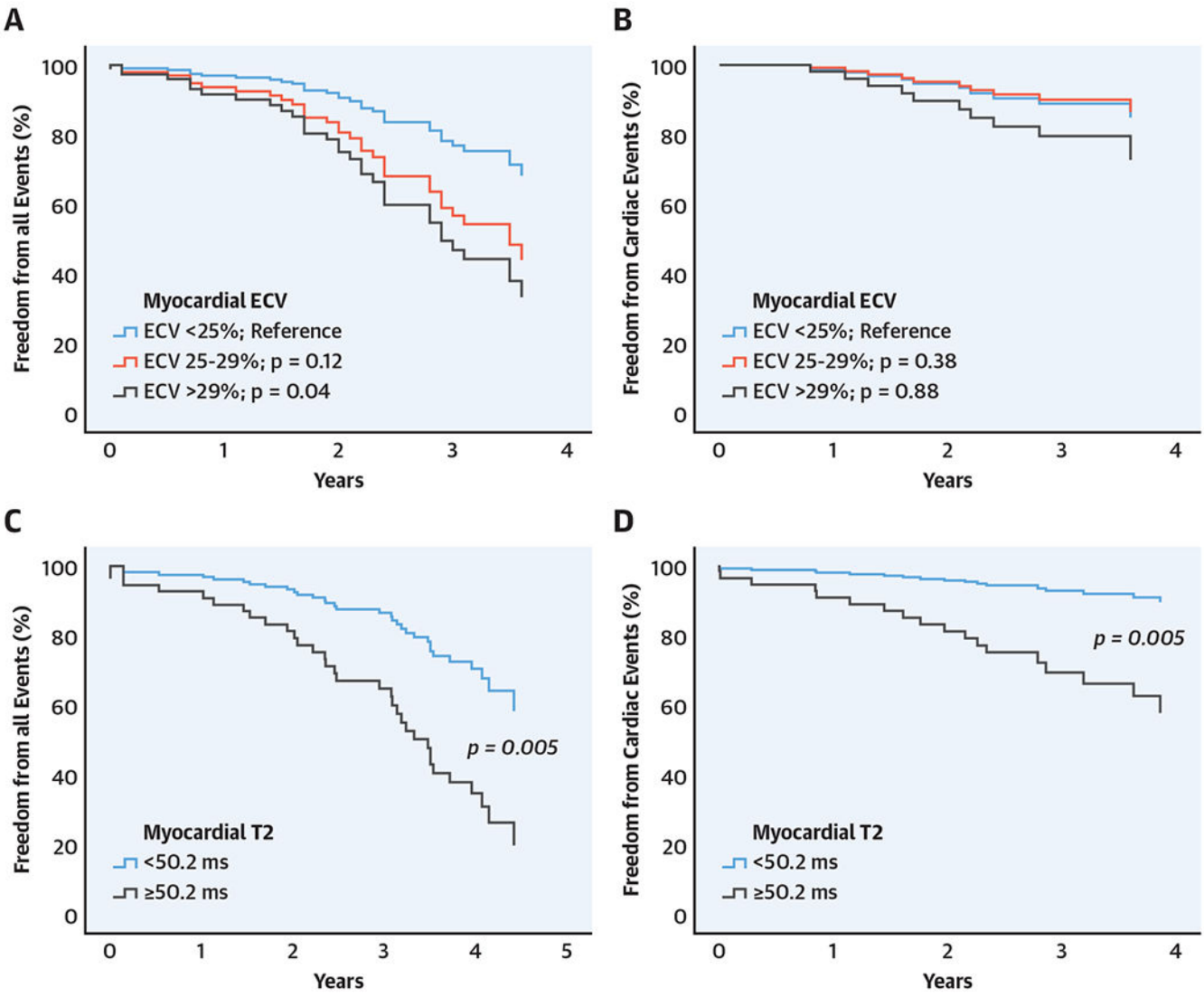

CENTRAL ILLUSTRATION. Survival Curves Categorized by Myocardial ECV and T2 Mapping

(A) Extracellular volume fraction (ECV) for all clinical events (covariates = left ventricular end systolic volume index [LVESVI], presence of late gadolinium enhancement [LGE]). **(B)** ECV for cardiac events (unadjusted). **(C)** T2 mapping for all clinical events (covariates = left ventricular ejection fraction [LVEF], LVESVI, presence of LGE). **(D)** T2 mapping for cardiac events (covariates = LVEF).

Author Manuscript Author Manuscript Author Manuscript Author Manuscript

JACC Cardiovasc Imaging. Author manuscript; available in PMC 2022 February 02.

TABLE 1

Patient Characteristics Categorized by ECV and T2

	Global ECV				Global T2		
	ECV <25% (1st tercile) (n = 29)	**ECV 25%-29% (2nd tercile) (n = 32)**	**ECV 29% (3rd tercile) (n = 29)**	**p Value**	**T2 <50.2 ms (T2 <median) (n = 39)**	**T2 ≥50.2 ms (T2 ≥median) (n = 40)**	**p Value**
Age, yrs	50 ± 17	51 ± 17	48 ± 14	0.69	52.8 ± 15.3	48.9 ± 15.6	0.12
Female	9 (31)	13 (41)	11 (38)	0.73	15 (39)	17 (43)	0.72
OHT-CMR interval, yrs	6.0 (3.5–8.3)	5.5 (3.0–8.0)	3.7 (0.5–7.6)	0.20	6.3 (3.9–9.1)	6.1 (4.0–8.6)	0.12
Any CAV	11 (39)	14 (45)	12 (44)	0.89	19 (49)	20 (50)	0.91
Hypertension	25 (86)	27 (84)	24 (83)	0.94	32 (82)	38 (95)	0.07
Dyslipidemia	20 (69)	17 (53)	10 (35)	0.03	24 (62)	21 (53)	0.42
Diabetes mellitus	11 (38)	10 (31)	9 (31)	0.82	15 (39)	10 (25)	0.20
History of rejection	4(14)	10 (31)	6 (21)	0.25	8 (21)	12 (30)	0.33
Antimetabolite	26 (90)	28 (88)	27 (93)	0.77	37 (95)	35 (88)	0.25
Antiproliferative	28 (97)	31 (97)	29 (100)	0.61	37 (95)	40 (100)	0.10
Steroid	11 (38)	9 (28)	16 (55)	0.10	12 (31)	10 (25)	0.75
Beta-blocker	7(24)	11 (34)	6 (21)	0.45	6 (15)	16 (40)	0.02
CCB	6 (21)	3 (9)	6 (21)	0.39	7 (18)	7 (18)	0.96
ARB	3 (10)	3 (9)	0 (0)	0.21	4 (10)	3 (8)	0.67
ACEI	13 (45)	12 (38)	14 (48)	0.68	22 (56)	20 (50)	0.57
Statin	27 (93)	29 (91)	27 (93)	0.92	36 (92)	35 (89)	0.48
Antiplatelet	27 (93)	26 (81)	26 (90)	0.34	31 (80)	37 (93)	0.10
Aldosterone antagonist	4 (14)	3 (9)	3 (10)	0.85	2 (5)	7 (18)	0.08

Author Manuscript Author Manuscript Author Manuscript Author Manuscript

	Global ECV				Global T2		
	ECV <25% (1st tercile) (n = 29)	**ECV 25%-29% (2nd tercile) (n = 32)**	**ECV 29% (3rd tercile) (n = 29)**	**p Value**	**T2 <50.2 ms (T2 <median) (n = 39)**	**T2 ≥50.2 ms (T2 ≥median) (n = 40)**	**p Value**
Diuretic	8 (28)	9 (29)	12 (41)	0.47	9 (23)	13 (33)	0.31
Presence of LGE	11 (38)	11 (34)	10 (35)	0.95	12 (34)	16 (46)	0.33
LGE extent,%	1.5 ± 2.5	1.4 ± 2.2	1.9 ± 4.6	0.81	1.3 ± 2.2	2.6 ± 4.4	0.14
Global native T1				0.25			0.54
1st tercile (<1,005 ms)	12 (41)	10 (31)	8 (28)		11 (31)	15 (43)	
2nd tercile (1,005-1,056 ms)	11 (38)	12 (38)	7 (24)		15 (43)	11 (31)	
3rd tercile (>1,056 ms)	6 (21)	10 (31)	14 (48)		9 (26)	9 (26)	
LVEF, %	58 ± 10	56 ± 9	57 ± 7	0.67	56.6 ± 7.8	56.9 ± 8.8	0.86
LVEDVI, ml/m^2	58 ± 13	63 ± 19	66 ± 16	0.18	59.8 ± 14.4	61.7 ± 16.1	0.60
LVESVI, ml/m^2	25 ± 9	26 ± 12	28 ± 9	0.46	26.1 ± 8.8	25.1 ± 8.2	0.58
LVSV, ml	64 ± 14	67 ± 21	73 ± 20	0.21	66.6 ± 19.1	66.9 ± 19.4	0.94
LVCO, ml	5.8 ± 1.2	5.8 ± 1.6	6.3 ± 1.9	0.33	5.6 ± 1.3	6.0 ± 1.8	0.27
LVMI, g/m^2	58 ± 18	56 ± 14	59 ± 17	0.81	56.1 ± 18.1	52.3 ± 13.3	0.31
RVEF, %	51 ± 8	50 ± 9	50 ± 8	0.88	50.2 ± 7.6	50.0 ± 9.1	0.93
RVEDVI, ml/m^2	65 ± 12	69 ± 15	24 ± 5	0.28	66.8 ± 15.5	70.6 ± 16.0	0.30
RVESVI, ml/m^2	33 ± 8	35 ± 10	16 ± 3	0.36	33.1 ± 9.1	36.0 ± 11.9	0.24
RHC-RAP, mm Hg	6 ± 4	10 ± 7	10 ± 7	0.03	7.6 ± 5.4	8.9 ± 6.1	0.33
RHC-RVSP, mm Hg	28 ± 8	34 ± 9	34 ± 10	0.02	30.1 ± 8.2	31.2 ± 9.1	0.38
RHC-RVDP, mm Hg	4 ± 3 *	7 ± 6 *	7 ± 5	0.02	5.5 ± 5.1	6.1 ± 4.9	0.63
RHC-PASP, mm Hg	27 ± 8	32 ± 11	33 ± 11	0.05	28.6 ± (8.2	30.0 ± 10.5	0.52
RHC-PADP, mm Hg	12 ± 6	16 ± 9	17 ± 8	0.06	13.3 ± 5.8	14.3 ± 8.2	0.54

JACC Cardiovasc Imaging. Author manuscript; available in PMC 2022 February 02.

Author Manuscript Author Manuscript Author Manuscript Author Manuscript

	Global ECV				Global T2		
	ECV <25% (1st tercile) (n = 29)	ECV 25%-29% (2nd tercile) (n = 32)	ECV 29% (3rd tercile) (n = 29)	p Value	T2 <50.2 ms (T2 <median) (n = 39)	T2 ≥50.2 ms (T2 ≥median) (n = 40)	p Value
RHC-mPAP, mm Hg	19 ± 6 *	23 ± 9	24 ± 9 *	0.04	20.3 ± 7.1	21.4 ± 8.1	0.54
RHC-PCWP, mm Hg	11 ± 5 *	14 ± 8	16 ± 8 *	0.01	11.8 ± 5.3	13.6 ± 8.0	0.23
RHC-CI, ml/m^2	3.2 ± 0.8	3.0 ± 0.8	2.9 ± 0.9	0.50	3.1 ± 1.0	3.0 ± 1.0	0.73

Values are mean ± SD, n (%), or median (interquartile range).

* Statistically significant with $p < 0.05$.

ACEI = angiotensin-converting enzyme inhibitor; ARB = angiotensin receptor blocker; CAV = cardiac allograft vasculopathy; CCB = calcium channel blocker; CI = cardiac index; ECV = extracellular volume; LVCO = left ventricular cardiac output; LGE = late gadolinium enhancement; LVEF = left ventricular ejection fraction; LVEDVI = left ventricular end-diastolic volume index; LVESVI = left ventricular end-systolic volume index; LVMI = left ventricular mass index; LVSV = left ventricular systolic volume; mPAP = mean pulmonary artery pressure; OHT-CMR = orthotropic heart transplant cardiovascular magnetic resonance imaging; PADP = pulmonary artery diastolic pressure; PASP = pulmonary artery systolic pressure; PCWP = pulmonary capillary wedge pressure; RAP = right atrial pressure; RHC = right heart catheterization; RVDP = right ventricular diastolic pressure; RVEDVI = right ventricular end-systolic volume index; RVEF = right ventricular ejection fraction; RVSP = right ventricular diastolic pressure; SD = standard deviation.

JACC Cardiovasc Imaging. Author manuscript; available in PMC 2022 February 02.

Author Manuscript

Author Manuscript

Author Manuscript

Author Manuscript

TABLE 2

Accuracy of Myocardial ECV and T2 Mapping for Clinical Outcomes

	Sensitivity	Specificity	Positive Predictive Value	Negative Predictive Value
ECV >29% for all events	38	71	41	67
ECV >29% for cardiac events	40	69	14	90
T2 >50.2 ms for all events	78	57	35	90
T2 >50.2 ms for cardiac events	68	66	65	69

Values are %. Abbreviation as in Table 1.

Author Manuscript Author Manuscript Author Manuscript Author Manuscript

TABLE 3

Multivariable Cox Regression Models of ECV for Clinical Events

Adjusted With CMR			Adjusted for Invasive Hemodynamics		
	Adjusted HR (95% CI)	**p Value**		**Adjusted HR (95% CI)**	**p Value**
Global ECV			Global ECV		
1st tercile (<25%)	1.00	Ref.	1st tercile (<25%)	1.00	Ref.
2nd tercile (25%-29%)	2.15 (0.82-5.59)	0.12	2nd tercile (25%-29%)	1.64 (0.61-4.42)	0.33
3rd tercile (>29%)	2.87 (1.07-7.68)	0.04	3rd tercile (>29%)	2.67 (0.93-7.64)	0.07
LVESVI	1.03 (1.00-1.06)	0.11	RHC-PCWP	1.06 (1.01-1.11)	0.03
Any LGE	2.40 (1.19-4.85)	0.02	RHC-CI	0.69 (0.43-1.12)	0.13

CI = confidence interval; HR = hazard ratio; RHC-CI = cardiac index by right heart catheterization; RHC-PCWP = pulmonary capillary wedge pressure by right heart catheterization; other abbreviations as in Table 1.

Author Manuscript

Author Manuscript

Author Manuscript

Author Manuscript

TABLE 4

Multivariable Cox Regression Models of T2 Mapping for Clinical Events

Adjusted With CMR			Adjusted for Invasive Hemodynamics		
	Adjusted HR (95% CI)	p Value		Adjusted HR (95% CI)	p Value
Cardiac events					
T2 ≥50.2 ms	4.92 (1.60-15.14)	0.005	T2 ≥50.2 ms	4.47 (1.25-15.99)	0.02
LVEF	0.94 (0.90-0.97)	0.001	RHC-PCWP	1.1 (1.00-1.10)	0.006
ALL clinical events					
T2 ≥50.2 ms	3.01 (1.39-6.54)	0.005	T2 ≥50.2 ms	2.69 (1.27-5.67)	0.01
LVEF	0.99 (0.94-1.04)	0.67	RHC-PCWP	1.05 (1.01-1.09)	0.03
Any LGE	1.94 (0.97-3.87)	0.06			
LVESVI	1.02 (1.00-1.04)	0.05			

Abbreviations as in Tables 1 and 3.